SPECTROSCOPY OF MOLECULAR HYDROGEN EMISSION FROM KH 15D[1]

Drake Deming

NASA Goddard Space Flight Center, Planetary Systems Branch, Code 693, Greenbelt, MD 20771; ddeming@pop600.gsfc.nasa.gov

David Charbonneau

California Institute of Technology, MS 105-24 (Astronomy), 1200 East California Boulevard, Pasadena, CA 91125; dc@caltech.edu

and

Joseph Harrington

Center for Radiophysics and Space Research, Cornell University, 326 Space Sciences Building, Ithaca, NY 14853-6801; jh@oobleck.astro.cornell.edu

ABSTRACT

We report infrared spectroscopy of the unusual eclipsing pre–main-sequence object KH 15D, obtained using NIRSPEC on Keck II. During eclipse, observations using low spectral resolution ($\lambda/\delta\lambda \sim 1000$) reveal the presence of prominent molecular hydrogen emission in five lines near 2 μm. The relative line strengths are consistent with thermal excitation at $T \sim 2800 \pm 300$ K. Observations out of eclipse, at both low and high spectral resolution ($\lambda/\delta\lambda \sim 2 \times 10^4$), show reduced contrast with the stellar continuum. The change in contrast for the strongest line, 1–0 $S(1)$, is consistent with an approximately constant emission line superposed on a variable stellar continuum. Emission in the 1–0 $S(1)$ line is observed to extend by $\gtrsim 4''$ both east and west of the stellar point-spread function (PSF; $\gtrsim 3000$ AU). Observed at high spectral resolution, the velocity and the intensity structure of the 1–0 $S(1)$ profile are both asymmetric. East of the stellar PSF (by $1''.1$–$2''.3$) the emission is blueshifted (-63 km s^{-1}) and has significantly greater intensity than the marginally redshifted component ($+2$ km s^{-1}, approximately consistent with zero) that dominates west of the stellar PSF. The spatial extent of the emission and the excitation temperature suggest shock excitation of ambient gas by a bipolar outflow from the star and/or the disk. However, it is difficult to account for the observed radial velocity unless the outflow axis is inclined significantly to the plane of the sky.

Subject headings: planetary systems: formation — planetary systems: protoplanetary disks — stars: pre–main-sequence

1. INTRODUCTION

KH 15D is a weak-lined T Tauri star (K7 V) in NGC 2264 ($d = 760$ pc), which shows deep (3.5 mag) periodic eclipses, each lasting for about 20 days, a large fraction of the 48.36 day period (Herbst et al. 2002; Herbst & Hamilton 2003). The eclipses occur abruptly, indistinguishable from obscuration by a "knife edge" (Herbst et al. 2002). During eclipse, the lack of reddening in the spectrum (Hamilton et al. 2001), and polarization that varies only weakly with wavelength (Agol et al. 2004), imply that the obscuring matter must be comprised of large particles. A consensus view to date is that the eclipses are caused by structure in a protoplanetary disk, fortuitously edge-on to our line of sight. Candidate structures include a density wave (Herbst et al. 2002), a vortex (Barge & Viton 2003), or a warp in the disk induced by planet-disk interactions (Agol et al. 2004; Winn et al. 2003). The considerable recent interest in KH 15D derives from the diagnostic potential inherent in the eclipse geometry and from the serendipity of finding a protoplanetary system whose structure suggests that planetary formation is actively occurring.

Although the eclipses in KH 15D are evidently caused by large solid particles, observations of the gaseous component may help us to deduce the nature of the system. Hamilton et al. (2003) observed double-peaked atomic hydrogen emission lines, indicative of a bipolar outflow. In this Letter we report

the spectroscopic discovery of 2 μm molecular hydrogen lines in emission, also showing a double-peaked structure indicative of outflow. This H$_2$ emission has been independently discovered by Tokunaga et al. (2004), by imaging in a narrowband filter. Molecular hydrogen emission is commonly observed from pre–main-sequence objects (Bachiller 1996), where it can be excited by fluorescence (Black & van Dishoeck 1987) or by shocks (Shull & Beckwith 1982), and has been well studied in many cases. H$_2$ observations should therefore help to relate KH 15D to other pre–main-sequence systems.

2. OBSERVATIONS

We observed KH 15D using the NIRSPEC spectrometer on the Keck II telescope (McLean et al. 1998). Observations on 2002 August 19 and 26 UT used NIRSPEC's low spectral resolution mode, with slit widths of $0''.76$ and $0''.57$, respectively, giving $\lambda/\delta\lambda \sim 1100$ and ~ 1500. KH 15D was in eclipse on August 19 (at phase = 0.17, emergence was just beginning; zero phase is center of eclipse) and out of eclipse on August 26 (phase = 0.32). Noise from the sky background was higher than usual on both nights because the object was observed at high air mass (~ 2) in predawn conditions, with a rapidly brightening sky. (KH 15D observations were supplementary to our main program.) Sky subtraction was facilitated by nodding the telescope to well-separated "a" and "b" positions along the slit. The position angle (P.A.) of the slit (measured positive eastward from north) and the total integration time used were $75°$ and 600 s and $134°$ and 400 s on August 19 and 26, respectively.

On 2002 September 2 UT, KH 15D was out of eclipse (phase = 0.46). We observed it using NIRSPEC's high-resolution cross-dispersed mode, giving $\lambda/\delta\lambda \sim 23,000$, with a
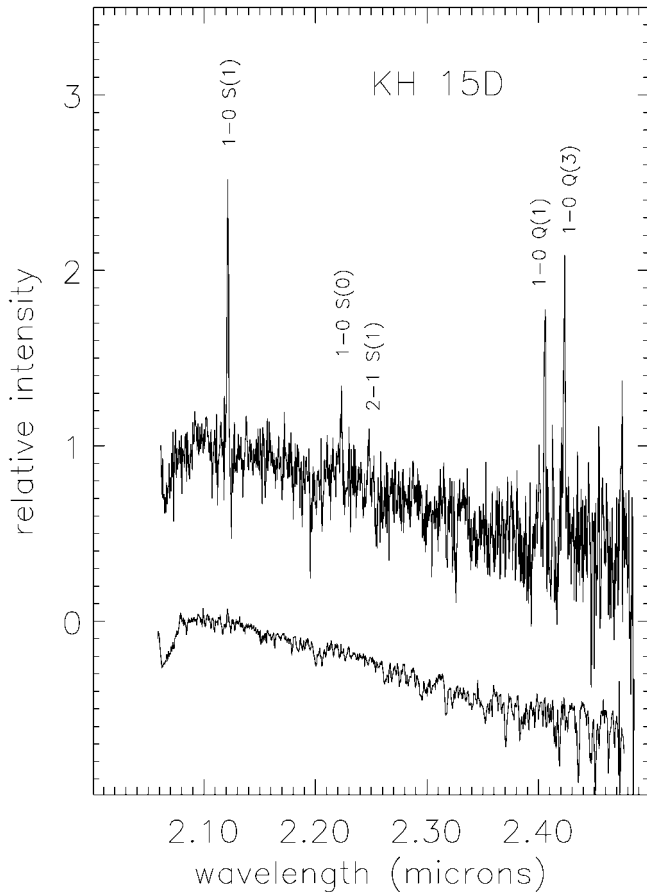
Fig. 1.—Keck/NIRSPEC low spectral resolution observations of KH 15D during eclipse (upper spectrum, 2002 August 19) and out of eclipse (lower spectrum, 2002 August 26). The lower spectrum has been offset downward by 1.0 for clarity. Five emission lines due to molecular hydrogen are identified and are much more prominent relative to the stellar continuum during eclipse. The absorption lines that are most apparent in the lower spectrum are telluric.

TABLE 1
Observed Line Intensities[a]

Line	Observed Intensity	Thermal Intensity ($T = 2800$ K)
1–0 $S(1)$	1.0	1.0
1–0 $S(0)$	0.30 ± 0.04	0.21
2–1 $S(1)$	0.24 ± 0.05	0.19
1–0 $Q(1)$	0.93 ± 0.09	0.71
1–0 $Q(3)$	0.94 ± 0.11	0.80

[a] Normalized to 1–0 $S(1)$ and compared with the intensities expected from thermal excitation at $T = 2800$ K.

0″.43 slit width (3 pixels) and P.A. = 66°. Total integration time was 1600 s. These high-resolution observations were made under better sky conditions (with an air mass of ~1.7) and also used nodding for sky subtraction. For both the low- and high-resolution spectra, we observed a neon emission lamp for wavelength calibration and a continuum lamp for flat-fielding.

3. SPECTRAL ANALYSIS

3.1. *Low-Resolution Spectra*

Sky and dark current subtraction was accomplished to first order by subtracting the *b* frames from the *a* frames, after division by the flat-field lamp frame. A second-order sky correction was accomplished by subtracting a residual sky spectrum from the average difference frame. The residual sky spectrum was determined on the average difference frame by summing a region located spatially between the *a* and *b* positions of the star on the slit. The KH 15D spectrum was obtained in a standard extraction, by summing both the *a* and *b* spectra over a region of ±2″ along the slit, after correction for the tilt of the slit. The wavelength scale was determined by fitting Gaussian profiles to 14 neon emission lines in calibration spectra taken immediately following the KH 15D spectra. The neon rest wavelengths (from the NIRSPEC manual) were expressed as a quadratic function of the fitted line positions (in

pixels), with coefficients determined by least squares. The precision of the wavelength calibration, estimated from the scatter in the quadratic fits, is ~0.0002 μm (0.5 pixels). Figure 1 shows the low-resolution spectra in and out of eclipse, with the wavelength scale transformed to the stellar frame. Our velocity transformations assume a heliocentric stellar radial velocity of +10 km s^{-1}, intermediate between the two values cited by Hamilton et al. (2003). Both spectra in Figure 1 have been flat-fielded and normalized to a unit intensity near 2.1 μm. We did not observe a standard flux source, but we were able to use the KH 15D stellar continuum to estimate an absolute line intensity (see below).

The low-resolution spectrum during eclipse shows five emission lines due to H$_2$, as noted in Figure 1. Even the weakest of these lines, 2–1 $S(1)$, is real, which we judged by inspecting the average difference frame prior to spectral extraction. On the difference frame, emission in the strongest line, 1–0 $S(1)$, has a spatial distribution along the slit that is peaked at the stellar position to within 0″.2 (1 pixel). This bright emission can be traced beyond the stellar point-spread function (PSF) by at least ±4″. There is evidence of faint $S(1)$ emission (with an intensity ~0.2 of the KH 15D peak) at one other position along the slit, ~16″ distant from KH 15D.

Intensities for the H$_2$ lines were determined by fitting Gaussian profiles. The widths of the fitted Gaussians were all constrained to equal the best-fit width for the 1–0 $S(1)$ line since the lines are not spectrally resolved. Errors in the line intensities (areas under the Gaussian fits) were estimated using a Monte Carlo procedure: we repeated the fits many times on "synthetic" lines having the same line parameters and noise levels as in the real data. All of the line intensities and errors are normalized to unit intensity for the 1–0 $S(1)$ line and are tabulated in Table 1. We used the very high spectral resolution atlas of Livingston & Wallace (1991), convolved to the ~25 km s^{-1} widths of the lines (see below), and measured the telluric absorption at the Doppler-shifted position of each line. At the observed geocentric Doppler shift and line width, none of the KH 15D lines are coincident with significant telluric lines; hence, any telluric corrections are negligible, even at 2 air masses.

The weakness of the 2–1 $S(1)$ line is indicative of thermal excitation since models of fluorescent emission predict an intensity for this line of ~0.5 relative to the 1–0 $S(1)$ line (Black & van Dishoeck 1987). It is clear from Figure 1 that the intensity of 2–1 $S(1)$ is substantially less than half of the 1–0 $S(1)$ line. To determine the excitation temperature, we computed ln (I/gA), where I is the Table 1 line intensity, g is the upper level statistical weight, and A is the Einstein A-value. For optically thin emission, ln (I/gA) is proportional to the energy of the emitting level, with a constant of proportionality of $-1/T$. We adopted the line parameters tabulated by Fernandes, Brand, & Burton (1997) and calculated $T \sim 2800 \pm 300$ K by least squares. The relative intensities expected from thermal excitation

at $T = 2800$ K are tabulated in Table 1 for comparison. The differences between these values and the observed intensities are somewhat greater than our estimated observational errors, but not so discrepant as to contradict thermal excitation.

3.2. *High-Resolution Spectra*

Figure 1 shows that the emission-line contrast is greatly reduced out of eclipse, similar to the effect seen in atomic emission lines by Hamilton et al. (2003). In the presence of shot noise from the stellar continuum, observation of the emission lines outside of eclipse is problematic at low spectral resolution. But the contrast for unresolved emission lines is proportional to spectral resolution, and we have been able to measure the 1–0 $S(1)$ line in high-resolution spectra outside of eclipse.

Our high-resolution spectra were extracted from an average difference image in a manner similar to the low-resolution spectra. However, the high-resolution spectra did not require a second-order sky subtraction, and we used night-sky emission lines for wavelength calibration. A velocity (wavelength) precision of 1.8 km s^{-1} (0.4 pixels) was achieved by using four night-sky lines, two on each side of the 1–0 $S(1)$ line, with vacuum wavelengths from Rousselot et al. (2000). We adopted the precise vacuum wavelength (2.1218356 μm) of the 1–0 $S(1)$ line from Bragg, Brault, & Smith (1982). Similar to the low-resolution in-eclipse spectra, our high-resolution spectra also show the emission extending well beyond the stellar PSF by $\gtrsim 4''$. We extracted three high-resolution spectra from the average difference frame, and these spectra are shown in Figure 2. The first spectrum (upper portion of Fig. 2) was extracted by summing along the slit within $\pm 0''.9$ of the star. Two other spectra were extracted over the interval $1''.1$–$2''.3$ from the star to the east and west (lower spectra in Fig. 2).

We examined the total intensity of the line seen in Figure 2 (*top spectrum, near the star*), compared with the line intensity seen near the star during eclipse. Using the stellar continuum as a reference, and adopting an eclipse depth of 3.1 mag at the epoch of the Figure 1 spectrum (phase = 0.17; Herbst et al. 2002), we compute the intensity expected in Figure 2 (out of eclipse) by scaling the Figure 1 (in eclipse) line intensity. Since the emission is extended, we allow for the different solid angles (slit widths times distance summed along the slit). On this basis we expect to see a line intensity about 25% less than is actually observed in Figure 2. This is certainly within the errors of the observations, and we conclude that the 1–0 $S(1)$ line intensity is approximately constant and is not eclipsed. The variation in H$_2$ emission-line contrast can be accounted for (within the errors) solely by changes in the stellar brightness.

The line profiles seen in Figure 2 show two components. Relative to the reference frame of the star, a blueshifted component appears at -63 km s^{-1}, and a redshifted component at $+2$ km s^{-1}. Within the errors, the redshifted component is consistent with zero velocity. Although the total intensity in the emission is peaked at the stellar position, the relative intensity of the blue- and redshifted components changes abruptly there. East of the star, the blueshifted component dominates, whereas the redshifted component prevails to the west. The components are relatively narrow, FWHM ~ 25 km s^{-1}.

We have estimated the absolute line intensity for the Figure 2 spectrum coincident with the stellar position, adding both components. Using the V magnitude reported by Hamilton et al. (2001), and the $V-K$ color normal to a K7 dwarf from Bessel & Brett (1988), we deduce a K magnitude for the star of 12.9, outside of eclipse. Adopting the zero-magnitude flux from Bessel & Brett
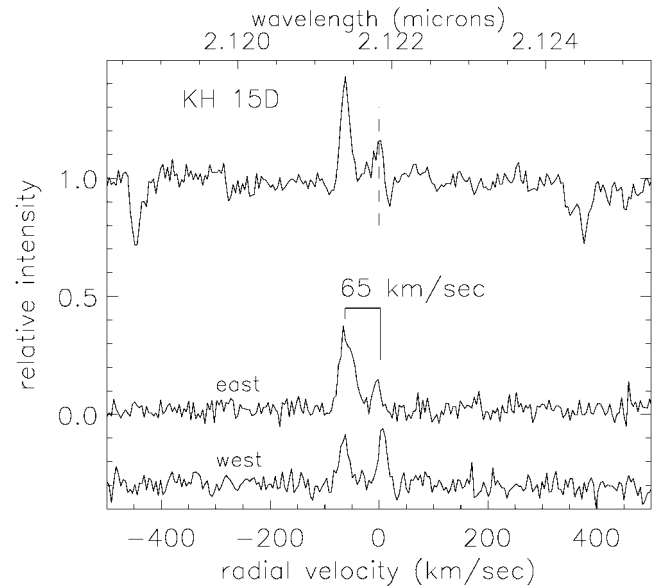

FIG. 2.—Keck/NIRSPEC high spectral resolution observations of KH 15D out of eclipse, showing double-peaked emission in the 1–0 $S(1)$ line. The upper spectrum was produced by integrating along the slit (oriented approximately east-west) by $\pm 0''.9$ from the star, so it shows the emission superposed on the stellar continuum. The absorption lines at -450 and $+370$ km s^{-1} are telluric. The two bottom spectra are offset east and west from the stellar position, both produced by integrating along the slit $1''.1$–$2''.3$ from the star. (The "west" spectrum has been offset downward by 0.3 for clarity.) The wavelength and radial velocity scales have been transformed into the rest frame of the star, where the dashed vertical line marks zero velocity.

(1988), we calculated the line intensity using the stellar continuum as a photometric standard. Since the star is a point source, whereas the emission is extended, we corrected for stellar slit losses. Fitting a Gaussian to the spatial profile of the star (along the slit), we derive $0''.8$ seeing (FWHM). Assuming image symmetry, a two-dimensional calculation indicates 21% loss at the slit ($0''.43$ slit width). We thereby derive a line intensity of $\sim 1.4 \times 10^{-16}$ ergs cm^{-2} s^{-1}. Following the calculation outlined by Bary, Weintraub, & Kastner (2003) for optically thin emission, this implies a mass $\sim 10^{-10}$ $M_\odot$ of hot H$_2$ and a column density of $\sim 6 \times 10^{14}$ molecules cm^{-2}. This is comparable to the hot H$_2$ mass in the near vicinity of several weak-lined T Tauri stars cited by Bary et al. (2003), except that we argue for shock heating by outflow in KH 15D, not UV fluorescence or heating by X-ray flux. Note that the inferred mass is proportional to the square of the source distance, and we have adopted $d = 760$ pc. Note also (see below) that Tokunaga et al. (2004) have imaged an extended jet of $S(1)$ emission, and the mass we derive here applies only to the immediate vicinity of the star (within $\pm 0.9 \times 0.43$ arcsec^2).

4. DISCUSSION

Tokunaga et al. (2004) have imaged KH 15D in a narrowband filter centered on the 1–0 $S(1)$ line. They find a prominent jet starting in close coincidence with the star and extending many arcseconds to the north. They have considered whether the jet is physically associated with KH 15D or whether it is a chance superposition (H$_2$ emission is common in star-forming regions like NGC 2264). Independent of our spectroscopy, they conclude that the association of the jet with KH 15D is probably physical. We find that (1) our low-resolution spectrum during eclipse shows bright $S(1)$ emission centered on the stellar position to $\sim 0''.2$ (§ 3.1) and (2) our high-resolution spectrum

resolves the line into two velocity components, whose relative intensities change abruptly at the stellar position (§ 3.2). Therefore, our results strongly support the conclusion that $S(1)$ emission is physically associated with KH 15D.

Recently, quiescent H_2 1–0 $S(1)$ emission has been detected near several T Tauri stars (Weintraub, Kastner, & Bary 2000; Bary et al. 2003). This quiescent emission shows narrow line profiles, just as we see in KH 15D. We considered the possibility that the KH 15D emission originates from quiescent gas, with Doppler shifts resulting from Keplerian orbital motion. We cannot exclude that some fraction of the emission, especially in the red component, arises from quiescent emission. Nevertheless, because the KH 15D emission is spatially extended and shows evidence of outflow, it seems more closely related to the shock-heated H_2 that has been observed in hundreds of young stellar objects, including classical T Tauri stars (Bachiller 1996; Herbst, Robberto, & Beckwith 1997).

Interpretation of our KH 15D observations requires knowing the stellar radial velocity, and the heliocentric radial velocity we adopt for the system ($+10$ km s^{-1}) may be in error if the star is a binary. Nevertheless, the double-peaked profiles we observe in the close vicinity of the star suggest outflow. However, a simple picture of a symmetric bipolar jet emergent normal to a single edge-on disk is hard to reconcile with our observations and with the Tokunaga et al. (2004) imaging. In such a simple interpretation, the line-of-sight shock velocity in the 1–0 $S(1)$ line would have to be at least half of the difference between the red- and blueshifted components, i.e., $\gtrsim 30$ km s^{-1}. For a disk inclination of $\sim 84°$ (Hamilton et al. 2003), the flow would be inclined by only $\sim 6°$ to the plane of the sky, so the total shock velocity would have to exceed ~ 250 km s^{-1}. This is well above the velocity where shocked H_2 is observed in other objects (H_2 becomes dissociated at high shock velocities; Shull & Beckwith 1982). Therefore, the outflow revealed in molecular hydrogen is likely to be inclined significantly to the plane of the sky. Similar arguments would not apply to lines formed very close to the star, where a bipolar outflow may not be collimated. However, the emission we observe is spatially resolved from the star, occurring at distances where bipolar outflows are often highly collimated to a single axis.

Tokunaga et al. (2004) find only one bright jet of line emission extending to the north. Since our slit was oriented primarily east-west (P.A. $= 66°$), we have observed approximately (but not precisely) perpendicular to the jet axis. Our spectra will reveal the flow pattern in the jet to the extent that the total angle between our slit and the velocity vector differs from $\pi/2$. We believe that our brightest emission component (the blueshifted "east" spectrum in Fig. 2) samples the Tokunaga et al. (2004) jet, whereas the red components are consistent with either a possible fainter counterjet (not yet detected by imaging) or quiescent emission near the stellar velocity.

The extent and complexity of H_2 emission from KH 15D are reminiscent of T Tauri itself, a known binary system. Consistent with its binary nature, T Tauri shows two nearly perpendicular outflow systems (Herbst et al. 1997). Our observations are not yet sufficient, in terms of spatial sampling, to say whether KH 15D shows a single or multiple velocity systems. Mapping spectroscopy of KH 15D in the 1–0 $S(1)$ line is needed to clarify the kinematics of this interesting object.

REFERENCES

Agol, E., Barth, A. J., Wolf, S., & Charbonneau, D. 2004, ApJ, 600, 781
Bachiller, R. 1996, ARA&A, 34, 111
Barge, P., & Viton, M. 2003, ApJ, 593, L117
Bary, J. S., Weintraub, D. A., & Kastner, J. H. 2003, ApJ, 586, 1136
Bessel, M. S., & Brett, J. M. 1988, PASP, 100, 1134
Black, J. H., & van Dishoeck, E. F. 1987, ApJ, 322, 412
Bragg, S. L., Brault, J. W., & Smith, W. H. 1982, ApJ, 263, 999
Fernandes, A. J. L., Brand, P. W. J. L., & Burton, M. G. 1997, MNRAS, 290, 216
Hamilton, C. M., Herbst, W., Mundt, R., Bailer-Jones, C. A. L., & Johns-Krull, C. M. 2003, ApJ, 591, L45
Hamilton, C. M., Herbst, W., Shih, C., & Ferro, A. J. 2001, ApJ, 554, L201
Herbst, T. M., Robberto, M., & Beckwith, S. V. W. 1997, AJ, 114, 744
Herbst, W., & Hamilton, C. M. 2003, in ASP Conf. Ser. 294, Scientific Frontiers in Research on Extrasolar Planets, ed. D. Deming & S. Seager (San Francisco: ASP), 231

Herbst, W., et al. 2002, PASP, 114, 1167
Livingston, W., & Wallace, L. 1991, An Atlas of the Solar Spectrum in the Infrared from 1850 to 9000 cm^{-1} (1.1 to 5.4 μm) (NSO Tech. Rep. 91-001; Tucson: NSO)
McLean, I. S., et al. 1998, Proc. SPIE, 3354, 566
Rousselot, P., Lidman, C., Cuby, J.-G., Moreels, G., & Monnet, G. 2000, A&A, 354, 1134
Shull, M. J., & Beckwith, S. 1982, ARA&A, 20, 163
Tokunaga, A. T., et al. 2004, ApJ, 601, L91
Weintraub, D. A., Kastner, J. H., & Bary, J. S. 2000, ApJ, 541, 767
Winn, J. N., Garnavich, P. M., Stanek, K. Z., & Sasselov, D. D. 2003, ApJ, 593, L121